ORGANISATION EUROPÉENNE POUR LA RECHERCHE NUCLÉAIRE

CERN-EP/89-168
December 19th, 1989

Search for Neutral Higgs Bosons from Supersymmetry in Z Decays

18 December 1989

The ALEPH Collaboration

D. Decamp, B. Deschizeaux, J.-P. Lees, M.-N. Minard

Laboratoire de Physique des Particules (LAPP), IN^{2}P^3-CNRS, 74019 Annecy-le-Vieux Cedex, France

J.M. Crespo, M. Delfino, E. Fernandez[1], M. Martinez, R. Miquel, Ll.M. Mir, S. Orteu, A. Pacheco, J.A. Perlas, E. Tubau

Laboratorio de Fisica de Altas Energias, Universidad Autonoma de Barcelona, 08193 Bellaterra (Barcelona), Spain[9]

M.G. Catanesi, M. de Palma, A. Farilla, G. Iaselli, G. Maggi, S. Natali, S. Nuzzo, A. Ranieri, G. Raso, F. Romano, F. Ruggieri, G. Selvaggi, L. Silvestris, P. Tempesta, G. Zito

INFN Sezione di Bari e Dipartimento di Fisica dell' Università, 70126 Bari, Italy

H. Hu, D. Huang, J. Lin, T. Ruan, T. Wang, W. Wu, Y. Xie, D. Xu, R. Xu, J. Zhang, W. Zhao

Institute of High-Energy Physics, Academia Sinica, Beijing, The People's Republic of China[10]

H. Albrecht[2], W.B. Atwood[3], F. Bird, E. Blucher, T.H. Burnett[4], T. Charity, H. Drevermann, Ll. Garrido, C. Grab, R. Hagelberg, S. Haywood, B. Jost, M. Kasemann, G. Kellner, J. Knobloch, A. Lacourt, I. Lehraus, T. Lohse, D. Lüke[2], A. Marchioro, P. Mato, J. May, A. Minten, A. Miotto, P. Palazzi, M. Pepe-Altarelli, F. Ranjard, A. Roth, J. Rothberg[4], H. Rotscheidt, W. von Rüden, R. St.Denis, D. Schlatter, M. Takashima, M. Talby, H. Taureg, W. Tejessy, H. Wachsmuth, S. Wheeler, W. Wiedenmann, W. Witzeling, J. Wotschack

European Laboratory for Particle Physics (CERN), 1211 Geneva 23, Switzerland

Z. Ajaltouni, M. Bardadin-Otwinowska, A. Falvard, P. Gay, P. Henrard, J. Jousset, B. Michel, J-C. Montret, D. Pallin, P. Perret, J. Proriol, F. Prulhière

Laboratoire de Physique Corpusculaire, Université Blaise Pascal, IN^{2}P^3-CNRS, Clermont-Ferrand, 63177 Aubière, France

J.D. Hansen, J.R. Hansen, P.H. Hansen, R. Møllerud, G. Petersen

Niels Bohr Institute, 2100 Copenhagen, Danmark[11]

E. Simopoulou, A. Vayaki

Nuclear Research Center Demokritos (NRCD), Athens, Greece

J. Badier, A. Blondel, G. Bonneaud, J. Bourotte, F. Braems, J.C. Brient, M.A. Ciocci, G. Fouque, R. Guirlet, A. Rougé, M. Rumpf, R. Tanaka, H. Videau, I. Videau[1]

Laboratoire de Physique Nucléaire et des Hautes Energies, Ecole Polytechnique, IN^{2}P^3-CNRS, 91128 Palaiseau Cedex, France

D.J. Candlin

Department of Physics, University of Edinburgh, Edinburgh EH9 3JZ, United Kingdom[12]

(Submitted to Physics Letters)

A. Conti, G. Parrini

Dipartimento di Fisica, Università di Firenze, INFN Sezione di Firenze, 50125 Firenze, Italy

M. Corden, C. Georgiopoulos, J.H. Goldman, M. Ikeda, J. Lannutti, D. Levinthal[17], M. Mermikides, L. Sawyer, G. Stimpfl

Supercomputer Computations Research Institute and Dept. of Physics, Florida State University, Tallahassee FL 32306, USA[14 15 16]

A. Antonelli, R. Baldini, G. Bencivenni, G. Bologna[5], F. Bossi, P. Campana, G. Capon, V. Chiarella, G. De Ninno, B. D'Ettorre-Piazzoli[6], G. Felici, P. Laurelli, G. Mannocchi[6], F. Murtas, G.P. Murtas, G. Nicoletti, P. Picchi[5], P. Zografou

Laboratori Nazionali dell'INFN (LNF-INFN), 00044 Frascati, Italy

B. Altoon, O. Boyle, A.W. Halley, I. ten Have, J.L. Hearns, I.S. Hughes, J.G. Lynch, W.T. Morton, C. Raine, J.M. Scarr, K. Smith[1], A.S. Thompson

Department of Physics and Astronomy, University of Glasgow, Glasgow G12 8QQ, United Kingdom[12]

B. Brandl, O. Braun, R. Geiges, C. Geweniger[1], P. Hanke, V. Hepp, E.E. Kluge, Y. Maumary, M. Panter, A. Putzer, B. Rensch, A. Stahl, K. Tittel, M. Wunsch

Institut für Hochenergiephysik, Universität Heidelberg, 6900 Heidelberg, Fed. Rep. of Germany[18]

A.T. Belk, R. Beuselinck, D.M. Binnie, W. Cameron[1], M. Cattaneo, P.J. Dornan, S. Dugeay, R.W. Forty, A.M. Greene, J.F. Hassard, S.J. Patton, J.K. Sedgbeer, G. Taylor, I.R. Tomalin, A.G. Wright

Department of Physics, Imperial College, London SW7 2BZ, United Kingdom[12]

P. Girtler, D. Kuhn, G. Rudolph

Institut für Experimentalphysik, Universität Innsbruck, 6020 Innsbruck, Austria[20]

C.K. Bowdery[1], T.J. Brodbeck, A.J. Finch, F. Foster, G. Hughes, N.R. Keemer, M. Nuttall, B.S. Rowlingson, T. Sloan, S.W. Snow

Department of Physics, University of Lancaster, Lancaster LA1 4YB, United Kingdom[12]

T. Barczewski, L.A.T. Bauerdick, K. Kleinknecht[1], B. Renk, S. Roehn, H.-G. Sander, M. Schmelling, F. Steeg

Institut für Physik, Universität Mainz, 6500 Mainz, Fed. Rep. of Germany[18]

J-P. Albanese, J-J. Aubert, C. Benchouk, A. Bonissent, D. Courvoisier, F. Etienne, E. Matsinos, S. Papalexiou, P. Payre, B. Pietrzyk[1], Z. Qian

Centre de Physique des Particules, Faculté des Sciences de Luminy, IN^2P^3-CNRS, 13288 Marseille, France

W. Blum, P. Cattaneo, G. Cowan, B. Dehning, H. Dietl, M. Fernandez-Bosman, D. Hauff, A. Jahn, E. Lange, G. Lütjens, G. Lutz, W. Männer, H-G. Moser, Y. Pan, R. Richter, A.S. Schwarz, R. Settles, U. Stiegler, U. Stierlin, J. Thomas, G. Waltermann

Max-Planck-Institut für Physik und Astrophysik, Werner-Heisenberg-Institut für Physik, 8000 München, Fed. Rep. of Germany[18]

V. Bertin, G. de Bouard, J. Boucrot, O. Callot, X. Chen, A. Cordier, M. Davier, G. Ganis, J.-F. Grivaz, Ph. Heusse, P. Janot, V. Journé, D.W. Kim, J. Lefrançois, A.-M. Lutz, J.-J. Veillet, F. Zomer

Laboratoire de l'Accéléateur Linéaire, Université de Paris-Sud, IN^2P^3-CNRS, 91405 Orsay Cedex, France

S.R. Amendolia, G. Bagliesi, G. Batignani, L. Bosisio, U. Bottigli, C. Bradaschia, I. Ferrante, F. Fidecaro, L. Foà[1], E. Focardi, F. Forti, A. Giassi, M.A. Giorgi, F. Ligabue, A. Lusiani, E.B. Mannelli, P.S. Marrocchesi, A. Messineo, F. Palla, G. Sanguinetti, S. Scapellato, J. Steinberger, R. Tenchini, G. Tonelli, G. Triggiani

Dipartimento di Fisica dell'Università, INFN Sezione di Pisa, e Scuola Normale Superiore, 56010 Pisa, Italy

J.M. Carter, M.G. Green, P.V. March, T. Medcalf, M.R. Saich, J.A. Strong[1], R.M. Thomas, T. Wildish

Department of Physics, Royal Holloway & Bedford New College, University of London, Surrey TW20 OEX, United Kingdom[12]

D.R. Botterill, R.W. Clifft, T.R. Edgecock, M. Edwards, S.M. Fisher, J. Harvey, T.J. Jones, P.R. Norton, D.P. Salmon, J.C. Thompson

Particle Physics Dept., Rutherford Appleton Laboratory, Chilton, Didcot, OXON OX11 OQX, United Kingdom[12]

E. Aubourg, B. Bloch-Devaux, P. Colas, C. Klopfenstein, E. Lançon, E. Locci, S. Loucatos, L. Mirabito, E. Monnier, P. Perez, F. Perrier, J. Rander, J.-F. Renardy, A. Roussarie, J.-P. Schuller

Département de Physique des Particules Élémentaires, CEN-Saclay, 91191 Gif-sur-Yvette Cedex, France[19]

J.G. Ashman, C.N. Booth, F. Combley, M. Dinsdale, J. Martin, D. Parker, L.F. Thompson

Department of Physics, University of Sheffield, Sheffield S3 7RH, United Kingdom[12]

S. Brandt, H. Burkhardt, C. Grupen, H. Meinhard, E. Neugebauer, U. Schäfer, H. Seywerd

Fachbereich Physik, Universität Siegen, 5900 Siegen, Fed. Rep. of Germany[18]

B. Gobbo, F. Liello, E. Milotti, F. Ragusa[7], L. Rolandi[1]

Dipartimento di Fisica, Università di Trieste e INFN Sezione di Trieste, 34127 Trieste, Italy

L. Bellantoni, J.F. Boudreau, D. Cinabro, J.S. Conway, D.F. Cowen, Z. Feng, J.L. Harton, J. Hilgart, R.C. Jared[8], R.P. Johnson, B.W. LeClaire, Y.B. Pan, T. Parker, J.R. Pater, Y. Saadi, V. Sharma, J.A. Wear, F.V. Weber, Sau Lan Wu, S.T. Xue, G. Zobernig

Department of Physics, University of Wisconsin, Madison, WI 53706, USA[13]

---

[1] Now at CERN.

[2] Permanent address: DESY, Hamburg, Fed. Rep. of Germany.

[3] On leave of absence from SLAC, Stanford, CA 94309, USA.

[4] On leave of absence from University of Washington, Seattle, WA 98195, USA.

[5] Also Istituto di Fisica Generale, Università di Torino, Torino, Italy.

[6] Also Istituto di Cosmo-Geofisica del C.N.R., Torino, Italy.

[7] Now at INFN Milano.

[8] Permanent address: LBL, Berkeley, CA 94720, USA.

[9] Supported by CAICYT, Spain.

[10] Supported by the National Science Foundation of China.

[11] Supported by the Danish Natural Science Research Council.

[12] Supported by the UK Science and Engineering Research Council.

[13] Supported by the US Department of Energy, contract DE-AC02-76ER00881.

[14] Supported by the US Department of Energy, contract DE-FG05-87ER40319.

[15] Supported by the NSF, contract PHY-8451274.

[16] Supported by the US Department of Energy, contract DE-FC0S-85ER250000.

[17] Supported by SLOAN fellowship, contract BR 2703.

[18] Supported by the Bundesministerium für Forschung und Technologie, Fed. Rep. of Germany.

[19] Supported by the Institut de Recherche Fondamentale du C.E.A..

[20] Supported by Fonds zur Förderung der wissenschaftlichen Forschung, Austria.

Abstract

The light scalar Higgs boson h and the pseudoscalar Higgs boson A of the Minimal Supersymmetric Standard Model have been searched for in the processes $e^+e^- \to hf\bar{f}$ and $e^+e^- \to hA$ using data collected by ALEPH at the LEP e^+e^- collider, with center of mass energies at and near the Z peak. Using a variety of signatures adapted to various mass ranges for h and A, we have excluded a large domain in the parameter space. For large values of v_2/v_1, the ratio of the vacuum expectation values of the two Higgs fields, the whole range from 0 to 38.8 GeV is excluded for M_h and M_A at 95% CL.

1.- Introduction.

In the Standard Model of electroweak interactions,[1] the spontaneous breakdown of the $SU(2)_L \times U(1)_Y$ symmetry to $U(1)_{EM}$ is achieved at the expense of the introduction of new scalar fields. One doublet of such complex fields is sufficient for the Higgs mechanism[2] to operate: the W and Z bosons acquire masses and, out of the four initial degrees of freedom, one survives in the form of a physical state, "the" Higgs boson H. This model has received impressive experimental confirmation, the most striking of which are the discoveries of the weak neutral currents[3] and of the W and Z bosons.[4] But its essential ingredient, the Higgs boson, has escaped detection until now, and a lower mass limit of 15 GeV has recently been set at LEP by ALEPH from the analysis of e^+e^- collisions at and near the Z^0 peak.[5]

In spite of its successes, the Standard Model suffers from a number of theoretical difficulties which make it commonly believed to be only a low energy approximation of a more fundamental theory. The Higgs boson mass, for instance, receives quadratically divergent contributions (this is known as the "hierarchy problem"), and the only known way to stabilize it is to introduce supersymmetry.[6] This, however, has consequences in the Higgs sector: at least two doublets of Higgs fields are necessary in order to obtain the anomaly cancellations, and also to give masses to both up and down type quarks.[7] Two doublets are also sufficient, and it is in this framework, the Minimal Supersymmetric Standard Model (MSSM), that we will place ourselves for the remainder of this letter.

With two complex doublets, five physical states are predicted to exist, with masses and couplings highly constrained by supersymmetry[8]: two charged Higgs bosons, with mass larger than M_W, one neutral scalar heavier than the Z, one neutral scalar h lighter than the Z, and one pseudoscalar A with mass larger than M_h. It is of course with the two latter states that we will be concerned. The only two parameters needed to completely describe the Higgs sector in the MSSM can conveniently be chosen as M_h and $\tan\beta = v_2/v_1$ (v_1 and v_2 are the vacuum expectation values of the two Higgs doublets), or alternatively M_h and M_A. In particular, the mixing angle α between the two neutral scalars is then determined.

If v_2 and v_1 are very close to each other, the h scalar behaves essentially like a standard Higgs boson H in its coupling to the Z^0 and in its decay modes. Such decay modes are dominated by the highest mass fermion pair which is kinematically accessible. However, as v_2/v_1 becomes different from unity, the hZZ coupling is reduced with respect to HZZ by a factor $\sin(\alpha-\beta)$, and therefore

$$\frac{\Gamma(Z \to hZ^*)}{\Gamma(Z \to HZ^*)} = \sin^2(\alpha-\beta). \qquad (1)$$

The $hf\bar{f}$ couplings are modified as well: if $v_2/v_1 > 1$, the $hd\bar{d}$ and $hl\bar{l}$ couplings are enhanced, and the $hu\bar{u}$ one reduced, by roughly a factor v_2/v_1; the reverse occurs if $v_2/v_1 < 1$. Taking these features into account, excluded domains in the $(M_h, v_2/v_1)$ plane

can be inferred from the mass limits previously obtained for a standard Higgs boson. Such an analysis will be presented in Section 3. The sensitivity of this method, however, is limited to v_2/v_1 values close to 1 where $\sin^2(\alpha-\beta)$ is maximum.

Fortunately, as v_2/v_1 gets very different from unity, two phenomena occur simultaneously[9] : the A mass decreases to approach M_h, and the ZAh coupling becomes large. Therefore, the $Z \to hA$ decay channel becomes substantial with a partial width, for light h and A, of

$$\frac{\Gamma(Z \to hA)}{\Gamma(Z \to \nu\bar{\nu})} = 0.5 \cos^2(\alpha-\beta). \qquad (2)$$

From (1) and (2) one can see that the processes $Z \to hZ^*$ and $Z \to hA$ are complementary. The decays of the A can be determined from the $Af\bar{f}$ couplings which turn out to be very close to the $hf\bar{f}$ ones. The ratio v_2/v_1 is usually expected to lie in the range 1 to 20, depending on the top quark mass.[10] With the recent bounds obtained on the latter,[11,12] values of v_2/v_1 substantially greater than one are favoured.

It is the purpose of the analyses presented in Sections 4 to 8 to search for signals of the $Z^0 \to hA$ decay. These have been performed using data collected by ALEPH at the Z^0 peak (91.3 GeV) and in a region within ± 3 GeV of it during the months of September to November 1989, in which a total of 18610 Z^0 decays to multihadrons have been identified as explained in Ref.13.

All the results reported in this letter have been obtained using the H0DECAY program[14] to compute and simulate the decays of h and A. The main ingredients of this program have been described in Ref.5 in the standard Higgs boson case. For the present analyses, the appropriate modifications of the various h and A couplings have been made to comply with the constraints of the MSSM.[15]

2.- The ALEPH detector.

A detailed description of ALEPH can be found in Ref.16. The parts of the detector relevant for the analyses reported in this letter are:

- an inner tracking chamber (ITC), providing up to 8 coordinates in azimuth and in radius from 13 to 29 cm of the beam axis,
- a large time projection chamber (TPC), extending to a radius of 180 cm, and providing up to 21 three-dimensional coordinates,
- the electromagnetic calorimeter (ECAL), the barrel part of which is located between the TPC and the solenoidal superconducting coil which delivers a 1.5 T magnetic field,
- the hadronic calorimeter (HCAL), the iron return yoke of the magnet which has been instrumented.

The apparatus was triggered independently by several conditions, of which the ones relevant here are:

- an energy deposit of at least 6.5 GeV in the barrel part of ECAL, or at least 3.8 GeV in one of the ECAL end caps, or at least 1.6 GeV in both of these end caps,
- an ITC track in coincidence in azimuth with an energy deposit of at least 1.3 GeV in ECAL,
- an ITC track in coincidence in azimuth with a signal of penetration of at least 40 cm of iron in HCAL.

The data were processed through a chain of reconstruction programs, the output of which is a set of charged tracks, of calorimeter clusters, and of relations between those.

3.- Results inferred from the standard Higgs boson search.

The ALEPH Collaboration has recently reported a search for the standard neutral Higgs boson H in which a mass range extending from 32 MeV to 15 GeV was excluded.[5]

For short lived Higgs bosons ($M_H > 2M_\mu$), the number of events expected in this search decreases from around 40 to 3.6 as M_H increases from $2M_\mu$ to 15 GeV (see Table I in Ref.5). With a 95% CL upper limit of 3.45 (which incorporates a 15% systematic error) on any standard Higgs signal, this means that the expected production cross section may be reduced by as much as a factor of 11, extending down to 1 depending on M_H, with this mass range still being excluded at 95% CL. As the cross section for h production in $e^+e^- \to hf\bar{f}$ is reduced by a factor $\sin^2(\alpha-\beta)$ with respect to that of the equivalent process for H production, this means in turn that $\sin^2(\alpha-\beta)$ can be restricted to have a value less than 0.1 to 1, depending on M_h. This translates into the excluded domain in the $(M_h, v_2/v_1)$ plane shown as A in Fig.1. This inference however relies one the assumption that the Higgs decay pattern is not modified in a way which would invalidate the Higgs search reported in Ref.5. We have verified that this assumption is indeed correct in the range of M_h and v_2/v_1 values that are of interest here.

This assumption does not remain true for $M_h < 2M_\mu$. The Higgs decay width to electrons is enhanced for $v_2/v_1 > 1$, and decreased for $v_2/v_1 < 1$. Furthermore, the decay width into $\gamma\gamma$, which turns out to be minute for the standard Higgs because of a fortuitous cancellation between bosonic and fermionic loops,[17] becomes non negligible when v_2/v_1 is different from unity. These two effects modify the lifetime and the electronic branching ratio of h with respect to those of H. We have therefore reinterpreted the analysis presented in Ref.5 and in which an e^+e^- pair emerging from a detached vertex was used as the signature of a long lived Higgs, taking into account the modifications in the h decay pattern discussed above. This results in the excluded domain shown as A in Fig.2.

4.- Search strategy for the $Z^0 \rightarrow hA$ decay.

The characteristic signatures of the process $Z^0 \rightarrow hA$ strongly depend on the values of M_h and v_2/v_1. This can be seen in Fig.1a where regions are defined in the plane of these parameters, corresponding to various dominant final states. We have optimized the search strategy to be most efficient in the domain not yet excluded in Section 3.

Let us first consider the theoretically favoured side $v_2/v_1 > 1$:

In Region I, h decays exclusively to e^+e^- or $\gamma\gamma$ with a typical lifetime of a few tens of picoseconds. This leads to a decay length in the meter range, and the characteristic signature is thus an e^+e^- pair emerging from a vertex well detached from the collision point. This search is presented in Section 5.

In Region II, both h and A have masses less than $2M_\tau$ and decay to low-multiplicity final states. The signature is back-to-back very low-multiplicity jets. In Region IV, both h and A have masses less than $2M_B$ and decay preferentially to τ pairs (decays to $c\bar{c}$ are suppressed for $v_2/v_1 > 1$). The signature therefore remains the same as in Region II. This also applies to Region III where only A decays to τ pairs. This analysis is described in Section 6.

In Region V, h still decays to τ pairs while, as $M_A > 2M_B$, A decays preferentially to $b\bar{b}$. The final state here is $\tau^+\tau^-$ jet-jet. In Region VI, both h and A have masses greater than $2M_B$. They therefore decay preferentially to $b\bar{b}$ pairs, leading to 4-jet final states. However, the branching ratio to τ pairs always remains substantial (more than 5%). It is therefore worth looking for $\tau^+\tau^-$ jet-jet final states in this region too, with a background substantially reduced with respect to the general 4-jet final state. These searches are reported in Sections 7 and 8.

For $v_2/v_1 < 1$, the same argument holds up to the $D\bar{D}$ threshold. However, from there on (Region VII), $c\bar{c}$ decays dominate over $\tau^+\tau^-$, and only the 4-jet signature remains. This search is particularly difficult in the mass range 4 to 15 GeV where the jets from the same Higgs are not well separated, and we have not performed it.

The simulation program we have used is a simple $Z^0 \rightarrow hA$ decay generator, with cross section and angular distribution as given in Refs.8 and 17. In all cases, we have processed the generated events in the standard ALEPH detailed detector simulation and reconstruction programs to measure the signal detection efficiency. The trigger simulation has been tuned to reproduce the measured efficiencies for Bhabha, $\mu^+\mu^-$, $\tau^+\tau^-$ and $q\bar{q}$ events. For the topologies with which we are concerned, the trigger efficiency is always well above 95%. The normalization is obtained from the number of multihadronic Z^0 decays observed in the data samples on which the present analyses were performed.

5.- Very light Higgs searches.

For $2M_e < M_h < 2M_\mu$, h decays to e^+e^- or to $\gamma\gamma$ with a lifetime such that the decay vertex may be well separated from the collision point. For instance, for $M_h = 100$ MeV and $v_2/v_1 = 3$, the h lifetime is 4.6 ps, leading to a decay length of 63 cm, with an electronic branching ratio of 96%. In Region I, the A mass is such that it decays either also to e^+e^- or $\gamma\gamma$ with some non negligible lifetime (a mass of 125 MeV, a lifetime of 1.5 ps, a decay length of 16 cm and an electronic branching ratio of 39% in our example), or exclusively to $\mu^+\mu^-$. We have therefore searched for events containing an energetic e^+e^- pair emerging from a vertex well separated from the main interaction point, with no further constraint on the topology of the rest of the event.

The criteria to select such detached e^+e^- pairs are given in detail in Ref.5. No event remains within the fiducial volume of the TPC for this search, that is with a vertex more than 40 cm away from the beam axis, and with an energy of the e^+e^- pair above 20 GeV. This leads to the excluded domains shown as B in Fig.2, with no gap left between them and the domain A excluded in Section 3.

Finally, if both h and A lifetimes become so long that they escape the detector without decaying, or if either decays to $\gamma\gamma$ while the other escapes the detector, or decays to $\gamma\gamma$, to e^+e^-, or to $\mu^+\mu^-$, these final states will not contribute to the total hadronic cross section as measured by ALEPH in Ref.13, and they will therefore be incorporated in the effective number of neutrinos deduced thereof. As outlined in Ref.12, from the ALEPH measurement $N_\nu = 3.01 \pm 0.16$,[18] one can exclude any abnormal non hadronic contribution of more than 0.27 neutrinos at 95% CL. This translates into the excluded domains shown as C in Fig.2.

Our low mass Higgs searches lose their sensitivity when $M_h <\sim 30$ MeV together with $v_2/v_1 <\sim 1.2$ to 2.7 and $>\sim 0.8$ to 0.37. However, this domain is unambiguously excluded, for $M_h > 2M_e$, by the result of an electron beam dump experiment.[19] This is shown in Fig.2. The small windows around $M_h = 5$ and 35 MeV and $v_2/v_1 = 0.4$ are actually excluded at 95% CL when one properly combines the results of the two experiments, and the small elongated domain at $0.37 < v_2/v_1 < 2.7$ and $M_h < 2M_e$ is excluded by the combined "axion searches" of Ref.20.

6.- Search in low-multiplicity final states.

For $2M_\mu < M_{h(A)} < 2M_\tau$, h (A) decays to low-multiplicity final states. Final states containing two charged particles contribute from 100% to 25% of the total as $M_{h(A)}$ increases in this range, while final states containing two or four charged particles represent at least 60% of the total in all of the range. The rest is mostly due to purely neutral final states. Requiring a two-prong decay for h or A, and a two or four-prong decay for the other retains at least 25% of all hA final states. This leads to an expectation of more than a hundred events with such a topology in all of Region II.

For $v_2/v_1 > 1$ and $2M_\tau < M_{h(A)} < 2M_B$, h (A) decays preferentially to $\tau^+\tau^-$ in Region IV (III and IV). Taking into account the known topological branching ratios of the τ,[21] we infer that the topology used for the search in Region II retains more than 50% of the events in all of regions III and IV, leading to an expectation of hundreds of events therein.

To select events having the aforementioned topology, we applied the following procedure to our data sample.

First "good tracks" are defined as tracks such that

- their $d_0 < 2.5$ cm and their $z_0 < 5$ cm.
  Here d_0 is the distance of closest approach to the interaction vertex of the track extrapolation in the plane perpendicular to the beam axis, and z_0 is the distance of the track extrapolation to the interaction vertex, measured parallel to the beam axis at the point where d_0 is defined.
- they have at least 4 coordinates in the TPC and
  at least 1 coordinate in the ITC and a momentum above 500 MeV/c,
  or at least 7 coordinates in the ITC and TPC taken together.

The analysis is restricted to such "good tracks" and a charged track multiplicity of 4 or 6 is required. These tracks are used to calculate the event sphericity axis which is required to be more than 25.8° away from the beam axis. The event is divided into two hemispheres with respect to the sphericity axis. In each of these hemispheres, the electric charge is required to be zero and the total energy of the charged tracks to be larger than 5 GeV. Finally, each charged track is required to have a momentum larger than 1 GeV/c.

Only one event survives, restricting any potential signal in our data sample to contribute fewer than 4.74 events at 95% CL. With an efficiency close to unity for all the topologies considered in this analysis, all of regions II, III and IV are unambiguously excluded.

In Region V and, to a lesser extent, in Region VI, 4-τ final states still represent a significant fraction of all hA decays. Using these 4-τ final states only, we have extended the analysis performed for Region IV into these regions, and have thus excluded all of Region V and some of Region VI. This excluded domain is shown as E in Fig.1b.

For $v_2/v_1 < 1$, the results obtained in Region II remain valid. Those obtained in Region III and IV do not apply for $M_A > 2M_D$ since $c\bar{c}$ becomes the dominant A decay mode, thereby spoiling the low multiplicity signature.

For $M_h < 2M_\mu$, the search for detached vertices decribed in Section 5 had become inefficient for too short lifetimes. However, in such a case, the tracks from the h decay tend to behave like "good tracks" coming from the main vertex, given the finite tolerance in our d_0 and z_0 cuts. The hA final state, with $h \to e^+e^-$ and $A \to e^+e^-$ or $\mu^+\mu^-$, depending on the A mass, may then exhibit a topology of the kind searched during the

analysis of Region II. We can therefore extrapolate the results obtained in that search into Region I, with appropriate care being taken of the finite h and A lifetimes and of their branching ratios to the unused $\gamma\gamma$ final state. This results in the excluded domains shown as D in Fig.2. It can be seen that, after this analysis has been included, no gap remains between Region II and the domains in Region I already excluded in Sections 3 and 5.

7.- Search in the $\tau^+\tau^-$ jet-jet topology.

This topology is well adapted to the search in Region VI, the only one remaining for $v_2/v_1 > 1$. Indeed, although $b\bar{b}b\bar{b}$ is the dominant final state therein, the branching ratio into $\tau^+\tau^-$ always remains larger than 5%, both for h and A, and the $\tau^+\tau^-$ jet-jet final state has a rather characteristic signature if the dominant one-prong τ decays are used.

To select events potentially coming from this final state, we have applied the following procedure, using only "good tracks" as defined in Section 6. The total charged track energy is required to exceed 25% of the center of mass energy.

A cluster algorithm is applied to define jets, in which particles or jets are merged if the invariant mass squared of their system, normalized to the square of the visible energy, is less than 0.002. This corresponds to an effective mass cut of about 4 GeV. A minimum of four jets, two of them at least containing only one track, is required. Let the two most energetic single track jets be called "τ's". These "τ's" are required to have opposite electric charges, their momenta to be larger than 2 GeV/c, and their directions to be more than 25.8° away from the beam axis.

These two "τ's" are removed, and the remaining system is boosted into its center of mass. The sphericity axis is calculated therein, two hemispheres are defined with respect to this axis, and all particles in one of these hemispheres are said to form a "jet". These two "jets" are boosted back into the overall center of mass. Their directions are required to be more than 25.8° away from the beam axis, and all "τ"-"jet" angles are required to exceed 25.8°.

From the directions of the two "τ's" and of the two "jets", and from the "jet" velocities, all 4-momenta are recalculated by imposing the overall energy-momentum conservation.[22] If any of the measured "τ" or "jet" energies is reduced by more than 30% in this process, the event is rejected. At least one of the "τ's" and at least one of the "jets" must have recalculated momenta larger than 20 GeV/c while the other "τ" and the other "jet" must both have recalculated momenta larger than 2.5 GeV/c.

At this point, we are left with 12 events, of which 8 have a "$\tau\tau$" mass $M_{\tau\tau} < 10$ GeV. There is no reason to keep such events as they would lie within Region V which we have already excluded in Section 6. The cut $M_{\tau\tau} > 10$ GeV (C_1) has therefore been applied. The 4 remaining events have a "jet-jet" mass M_{jj} large with respect to $M_{\tau\tau}$, as can be seen in Fig.3. Indeed, this feature is expected from the QCD background whereas, for h and A masses well above $2M_B$, there are essentially as many "chances" a priori that

$M_{\tau\tau} > M_{jj}$ as the reverse. We have thus required in addition $M_{jj} - M_{\tau\tau} < 15$ GeV (C_2). Using a sample of hadronic events simulated with the program JETSET 6.3[23] which has been shown to reproduce ALEPH data accurately,[24] we find that, in the amount of data used for this search, we should expect 5.4 events after (C_1) and 1.8 ± 1.0 after C_2.

No event survives in the data sample, while the typical efficiency of the whole procedure is 25% for events from $Z^0 \to hA \to \tau^+\tau^- X$, with both τ's decaying to one prong. This allows us to exclude a large domain of Region VI, shown as F in Fig.1b. An alternate presentation of this result in terms of M_h and M_A is given in Fig.4 for $v_2/v_1 > 1$.

8.- Search in the 4-jet topology.

For h or A masses well above $2M_B$ and for $v_2/v_1 > 1$, $b\bar{b}$ is the dominant decay mode with a branching ratio of almost 95%. Four-jet final states will therefore dominate in $Z^0 \to hA$ decays when both h and A masses are large as in Region VI. However, the drawback of a search based on this topology comes from the large background of four-jet events from standard QCD production. Therefore, this method should be considered complementary to that described in Section 7 in which the expected signal rate was substantially lower but the background negligible.

For this analysis, we have used the class of events selected as Z^0 multihadronic decays as described in Ref.13. Such events must contain at least five "good tracks", and have a total energy in "good tracks" exceeding 10% of the center-of-mass energy. Here a "good track" is defined as one having $d_0 < 2$ cm and $z_0 < 10$ cm, making an angle with the beam axis greater than 18.2°, and having at least four coordinates in the TPC.

Events with a sphericity less than 0.03 or with an aplanarity less than 0.01 are removed first. A clustering algorithm[25] is then used to group the charged particles into four and only four jets. Events containing a jet with an energy less than 4 GeV or with a direction within 10° of the beam axis are removed. From the measured velocities of the four jets, the 4-momenta are then recalculated in the same way as in Section 7.

For each of the three possible jet-jet pairings, let i, j, k, l denote the four jet ordering, and let $\{ij\}$ and $\{kl\}$ form two jet pair systems (JPSs). The following quantities are then calculated:

- the invariant masses M_{ij} and M_{kl} of the two JPSs,
- the production angle, defined as the smaller of the two angles between the JPS directions and the beam axis,
- the two decay angles (one per JPS), each defined, in the JPS center of mass, as the angle between the common jet direction and the JPS direction,
- the two opening angles (one per JPS), each defined, in the overall center of mass, as the angle between the two jets of the JPS.

The $Z^0 \rightarrow hA$ decays obey a $\sin^2\theta$ angular distribution. This is in contrast to standard $q\bar{q}$ production and we therefore required that the production angle be greater than 60°. The $h(A)$ decays are also expected to be isotropic in the $h(A)$ rest frame. This is in contrast to gluon radiation from quarks. We therefore required that both decay angles be greater than 53.1°.

With four b quarks in the final state, the signal should show an abundance of leptons from semi-leptonic decays. We have therefore required the presence of at least one lepton with momentum greater than 3 GeV/c to enrich our sample. Electrons are identified with 90% efficiency over all of the "good track" acceptance using their characteristic shower pattern in ECAL. Muons are identified with 85% efficiency from their penetration in the iron of HCAL (only the barrel part was used for this analysis). These identification efficiencies have been measured in events from Z^0 decays.

In the region of interest in the (M_A, M_h) plane, the event topology can vary widely from essentially two-jet-like for low $\{M_A, M_h\}$ combinations to nearly isotropic for high $\{M_A, M_h\}$ combinations. For this reason, points distant in the (M_A, M_h) plane cannot be treated identically, but neighboring points are similar enough to permit the following procedure.

For a given $\{M_A, M_h\}$ combination, a region $\mathcal{R}$ in the mass plane is defined by $\{M_A \pm 5$ GeV, $M_h \pm 5$ GeV$\}$. All cuts are applied and, in addition, both opening angles are required to lie within a range of values defined by a parametrization linear in $\{M_A, M_h\}$ and optimized to discriminate simulated signal events against the standard QCD background, as shown in Fig.5.

In the data, one then counts how many events N_o are observed in $\mathcal{R}$. From events simulated using the same QCD Monte Carlo as in Section 7, one obtains μ_b, the expected number of background events in $\mathcal{R}$. From events simulated according to $Z^0 \rightarrow hA$, one estimates μ_s, the expected number of signal events in $\mathcal{R}$. From N_o and μ_b, one can then calculate the 95% CL upper limit μ_l on a signal, and compare it to μ_s. The $\{M_A, M_h\}$ combination considered is excluded if $\mu_s > \mu_l$. For instance, for $M_A = M_h = 30$ GeV, $\mu_s = 25.6$ (corresponding to an overall efficiency of the procedure of 8%) while $N_o = 9$ and $\mu_b = 4.3$, leading to $\mu_l = 11.4$; this mass combination is thus excluded.

If the (M_A, M_h) plane is divided into a suitably large number of sufficiently overlapping regions (0.5 GeV steps were chosen here), one can construct a smooth contour delineating a 95% CL excluded domain. This is shown as G in Fig.1b and 4. This contour has been obtained taking into account a conservative 20% systematic uncertainty on the values of μ_b, and has been verified insensitive to reasonable variations of the various cut values used in this analysis.

9.- Summary and conclusions.

In this letter, we have searched for signals for the production of the light scalar h and of the pseudoscalar A neutral Higgs bosons of the Minimal Supersymmetric Standard Model. Within the space of the parameters of the model (M_h and v_2/v_1, or M_h and M_A), we have used a variety of methods, each adapted to a specific region, and in this way we exclude a large domain of the range kinematically accessible in $Z^0 \rightarrow hA$ decays.

For very light h, we have taken advantage of the long h lifetime in a search for e^+e^- pairs emerging from a detached vertex. For intermediate mass h and A, we have used the low charged multiplicity characteristic of Higgs decays up to the $b\bar{b}$ or $c\bar{c}$ threshold, depending whether $v_2/v_1 >$ or < 1. For higher masses, we have looked for events consistent with either h or A decaying to $b\bar{b}$ with the opposite one decaying to $\tau^+\tau^-$ or $b\bar{b}$ (this applies only for $v_2/v_1 > 1$).

These negative searches, taken together with the results inferred from our previous limits on the standard Higgs boson production and from our measurement of the total hadronic cross section, lead to excluded domains as shown in Figs.1, 2 and 4. In particular, $M_h < 3.1$ GeV is excluded for any value of v_2/v_1 ; and, for v_2/v_1 substantially greater than unity as presently theoretically favoured, $M_h \simeq M_A$ is excluded up to 38.8 GeV.

To our knowledge, besides Refs.19 and 20 which deal with very low Higgs masses, the only previous result related to the subject discussed in this letter is that in Ref.26 which describes a search for $\Upsilon \rightarrow h\gamma$, a process which is known to be subject to serious uncertainties in the QCD radiative corrections. Our present results fill the gap between those of Refs.19 and 26, and considerably extend the excluded domain to higher Higgs masses.

Acknowledgements.

We wish to congratulate and thank our colleagues in the LEP Division for the extraordinary start-up performance of the LEP accelerator. We thank also the engineers and technicians in all our institutions for their support in constructing ALEPH. Those of us from the non-member countries thank CERN for its hospitality.

References.

1. S.L. Glashow, Nucl. Phys. **22** (1961) 579;
   S. Weinberg, Phys. Rev. Lett. **19** (1967) 1264;
   A. Salam, Proc. 8th Nobel Symp., ed. N. Svartholm (Almqvist and Wiksell, Stockholm, 1968) 367.
2. F. Englert and R. Brout, Phys. Rev. Lett. **13** (1964) 321;
   P.W. Higgs, Phys. Lett. **12** (1964) 132; Phys. Rev. Lett. **13** (1964) 508;
   Phys. Rev. **145** (1966) 1156;
   G.S. Guralnik, C.R. Hagen and T.W.B. Kibble, Phys. Rev. Lett. **13** (1964) 585;
   T.W.B. Kibble, Phys. Rev. **155** (1967) 1554.
3. F.J. Hasert et al. (GARGAMELLE Coll.) Phys. Lett. **46B** (1973) 121; **46B** (1973) 138;
   A. Benvenuti et al. (HPWF Coll.) Phys. Rev. Lett. **32** (1974) 800.
4. G. Arnison et al. (UA1 Coll.), Phys. Lett. **122B** (1983) 103;
   M. Banner et al. (UA2 Coll.), Phys. Lett. **122B** (1983) 476;
   G. Arnison et al. (UA1 Coll.), Phys. Lett. **126B** (1983) 398;
   P. Bagnaia et al. (UA2 Coll.), Phys. Lett. **129B** (1983) 130.
5. D. Decamp et al. (ALEPH Coll.), CERN-EP/89-157.
6. E. Witten, Nucl. Phys. **B188** (1981) 513;
   S. Dimopoulos and H. Georgi, Nucl. Phys. **B193** (1981) 150;
   N. Sakai, Z. Phys. **C11** (1981) 153.
7. K. Inoue et al., Prog. Theor. Phys. **67** (1982) 927 (E: **70** (1983) 330); **71** (1984) 413;
   See also Ref.6.
8. J.F. Gunion and H.E. Haber, Nucl. Phys. **B272** (1986) 1; **B278** (1986) 449;
   and earlier references therein.
9. G.F. Giudice, Phys. Lett. **208B** (1988) 315.
10. G.F. Giudice and G. Ridolfi, Z. Phys. **41C** (1988) 447;
    M. Olechowski and S. Pokorski, Phys. Lett. **214B** (1988) 393.
11. C. Albajar et al. (UA1 Coll.), Z. Phys. **C37** (1988) 505, as updated in G. Altarelli et al., Nucl. Phys. **B308** (1988) 724;
    F. Abe et al. (CDF Coll.), UPR-0172E (1989);
    T. Åkesson et al. (UA2 Coll.), CERN-EP/89-152;
    G.S. Abrams et al. (MARK II Coll.), SLAC PUB-5106 (1989);
    M.Z. Akrawy et al. (OPAL Coll.), CERN-EP/89-154.
12. D. Decamp et al. (ALEPH Coll.), "Search for New Quarks and New Charged and Neutral Leptons from Z^0 Decay at LEP", in preparation.
13. D. Decamp et al. (ALEPH Coll.), Phys. Lett. **231B** (1989) 519.
14. P. Janot, LAL 88-71 (1988).
15. P. Janot, LAL 89-45 (1989).
16. D. Decamp et al. (ALEPH Coll.), "ALEPH - A detector for electron-positron annihilation at LEP", to be submitted to Nucl. Inst. and Methods.
17. P.J. Franzini et al., Z Physics at LEP, eds. G. Altarelli, R. Kleiss and C. Verzegnassi, CERN 89-08.

18. D. Decamp et al. (ALEPH Coll.), "A precise determination of the number of families with light neutrinos and of the Z boson partial widths", in preparation.
19. M. Davier and H. Nguyen Ngoc, Phys. Lett. **229B** (1989) 150.
20. M. Sivertz et al., (CUSB Coll.), Phys. Rev. **D26** (1982) 717;
C. Edwards et al., (Crystal Ball Coll.), Phys. Rev. Lett. **48** (1982) 903.
21. Particle Data Group, Phys. Lett. **204B** (1988) and references therein
22. S.L. Wu, Z. Phys. **C9** (1981) 329
23. M. Bengtsson and T. Sjöstrand, Phys. Lett. **185B** (1987) 435;
B. Bambah et al., Z Physics at LEP, eds. G. Altarelli, R. Kleiss and C. Verzegnassi, CERN 89-08.
24. D. Decamp et al. (ALEPH Coll.), CERN-EP/89-139.
25. T. Sjöstrand, Comput. Phys. Comm. **28** (1983) 229.
26. J. Lee-Franzini (CUSB Coll.), Proc. of the XXIVth Int. Conf. on High Energy Physics, Munich, eds. R. Kotthaus and J.H. Kühn (Springer Verlag, 1988).

Figure Captions.

1. (a) In the $(v_2/v_1, M_h)$ plane:

   (A) : domain excluded by the searches for $e^+e^- \to hf\bar{f}$ (see Section 3 and Ref.5),

   (K) : the domain kinematically accessible in $Z^0 \to hA$ decays.

   In the domain complementary to (A), the various search regions defined according to characteristic final states in the process $Z^0 \to hA$ (see Section 4):

   (I) : $M_h < 2M_\mu$,

   (II) : $2M_\mu < M_h, M_A < 2M_\tau (2M_D)$ for $v_2/v_1 > 1 (< 1)$,

   (III) : $2M_\mu < M_h < 2M_\tau$ and $2M_\tau < M_A < 2M_B$,

   (IV) : $2M_\tau < M_h, M_A < 2M_B$,

   (V) : $2M_\tau < M_h < 2M_B$ and $2M_B < M_A$,

   (VI) : $2M_B < M_h, M_A$,

   (VII) : $2M_D < M_A$.

   (b) Excluded domains in the $(v_2/v_1, M_h)$ plane from:

   (A) : searches for $e^+e^- \to hf\bar{f}$ (see Section 3),

   (B) : final states with detached vertices in $Z^0 \to hA$ (see Section 6),

   (C) : the total hadronic cross section at the Z^0 peak (see Section 6),

   (D) : low multiplicity final states in $Z^0 \to hA$ (see Section 6),

   (E) : low multiplicity final states in $Z^0 \to hA$ (see Section 6),

   (F) : $\tau^+\tau^-$ jet-jet final states in $Z^0 \to hA$ (see Section 7),

   (G) : 4-jet final states in $Z^0 \to hA$ (see Section 8),

   (K) is the domain kinematically accessible in Z^0 decays.

   Altogether, ALEPH exclude the hatched region.

2. For very light Higgs bosons, excluded domains in the $(v_2/v_1, M_h)$ plane.
   The various domains are defined as in Fig.1b.
   Altogether, ALEPH exclude the hatched region. Also indicated, the domain excluded in Ref.19.

3. In the $\tau^+\tau^-$ jet-jet final state, the jet-jet mass M_{jj} vs. the $\tau\tau$ mass $M_{\tau\tau}$, after all cuts but C_1 and C_2 (see Section 7).

4. For $v_2/v_1 > 1$, excluded domains in the (M_A, M_h) plane from:

   (A) : searches for $e^+e^- \to hf\bar{f}$ (see Section 3),

   (E) : low multiplicity final states in $Z^0 \to hA$ (see Section 6),

   (F) : $\tau^+\tau^-$ jet-jet final states in $Z^0 \to hA$ (see Section 7),

   (G) : 4-jet final states in $Z^0 \to hA$ (see Section 8).

   Altogether, ALEPH exclude the hatched region. The region $M_A < M_h$ is forbidden theoretically.

5. In the 4-jet final state, the jet-jet opening angle for all events such that M_{ij} and M_{kl} fall within 30 ± 5 GeV (see Section 8) for:

   (a) the data,

   (b) events simulated using a QCD Monte Carlo,

   (c) events simulated using a $Z^0 \to hA \to b\bar{b}b\bar{b}$ Monte Carlo for $M_h = M_A = 30$ GeV.

   The arrows indicate the cut positions.

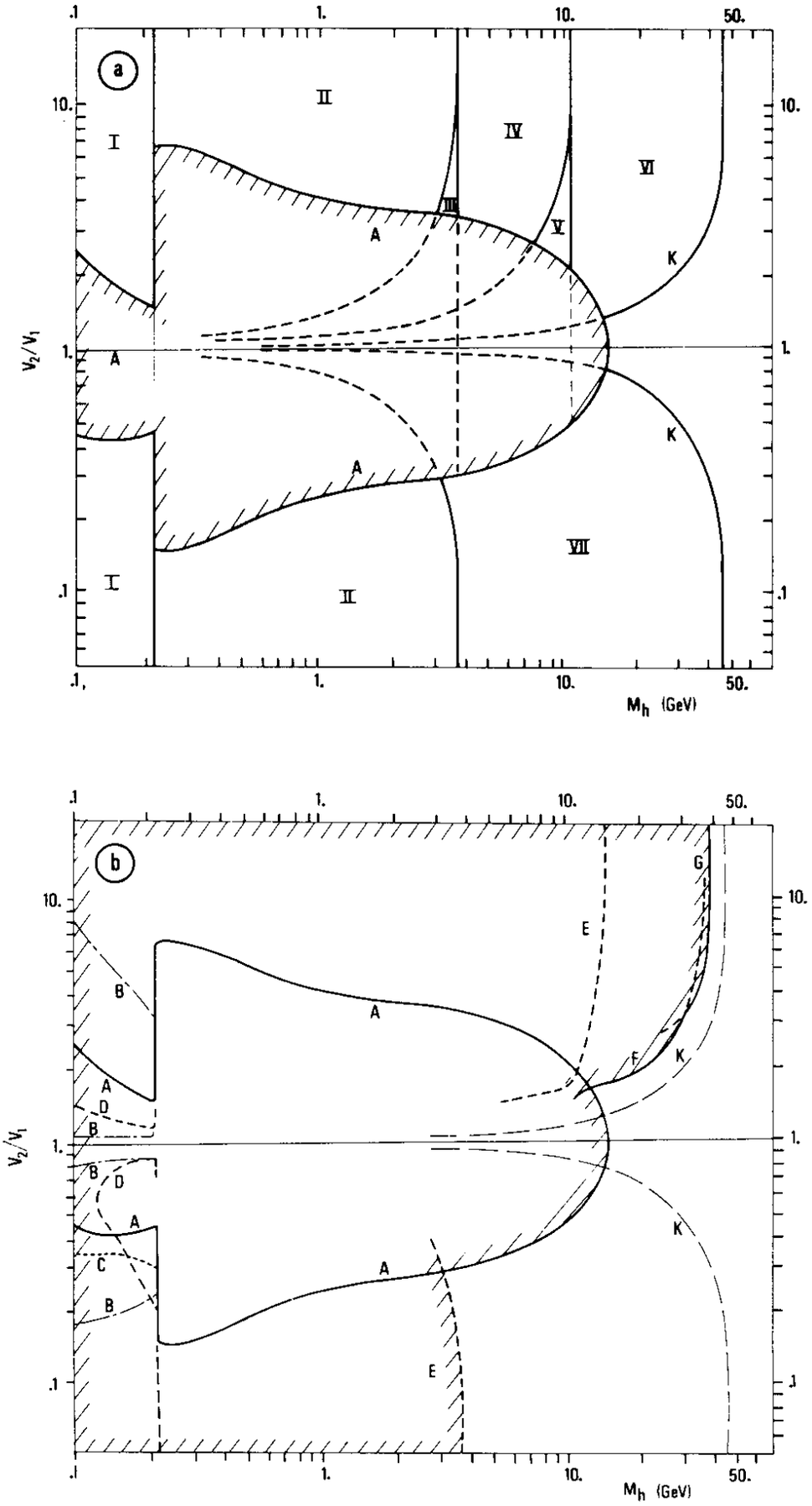

Figure 1.

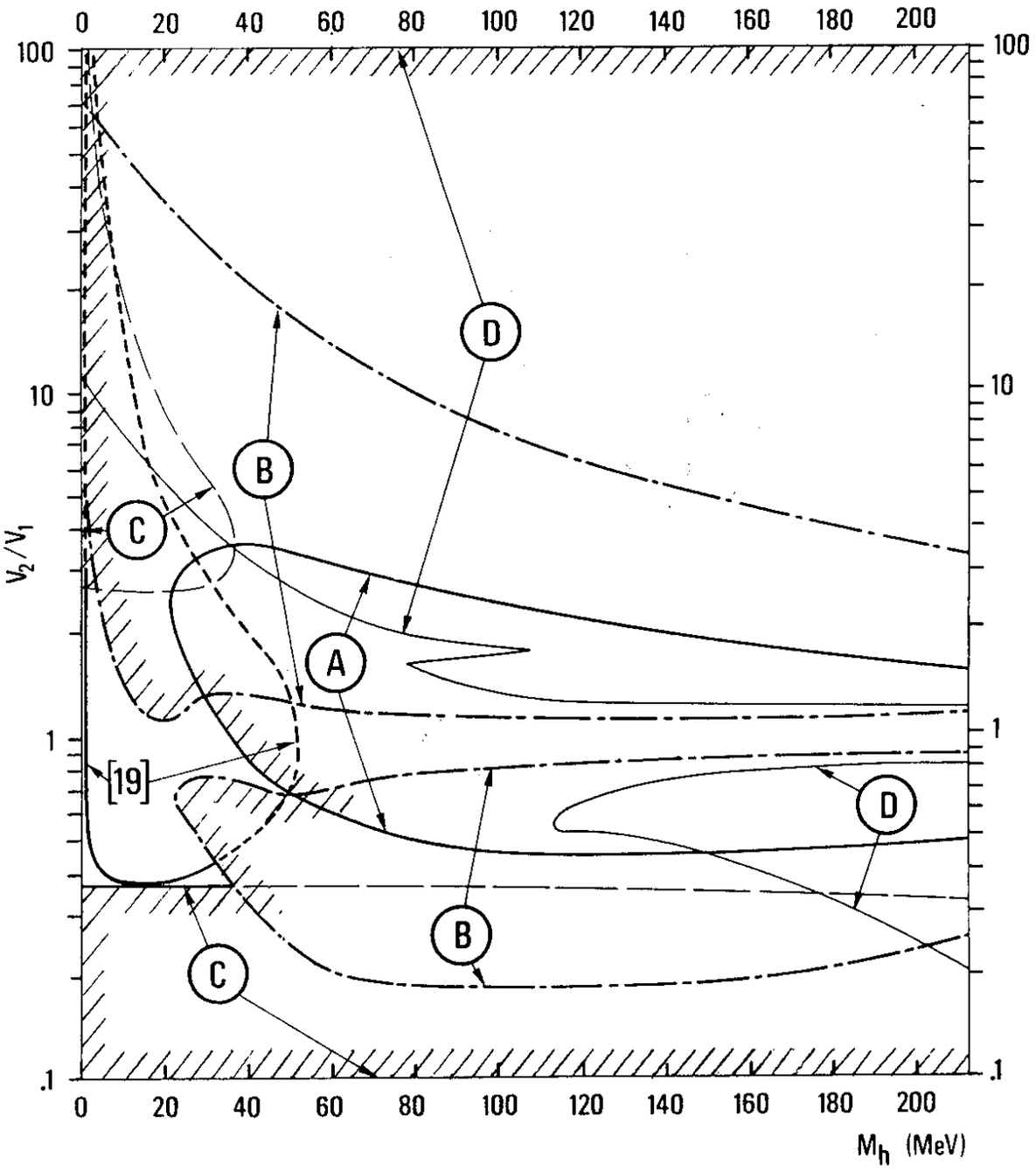

Figure 2.

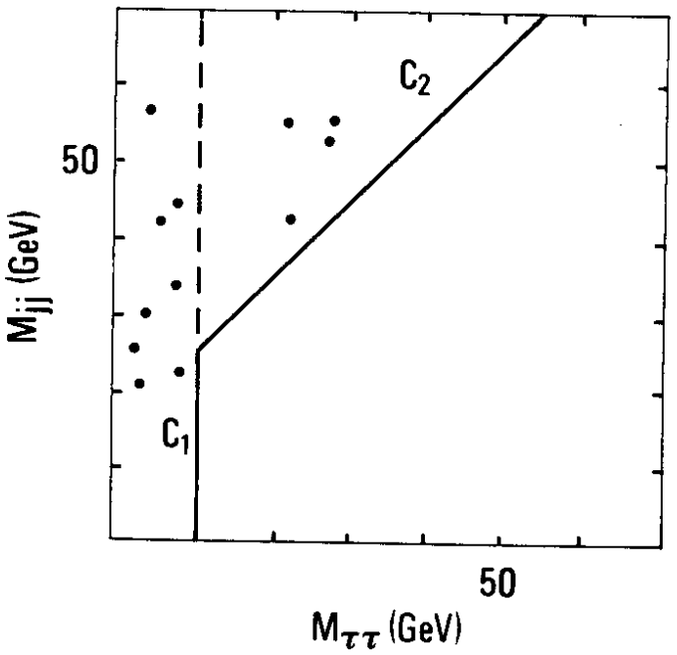

Figure 3.

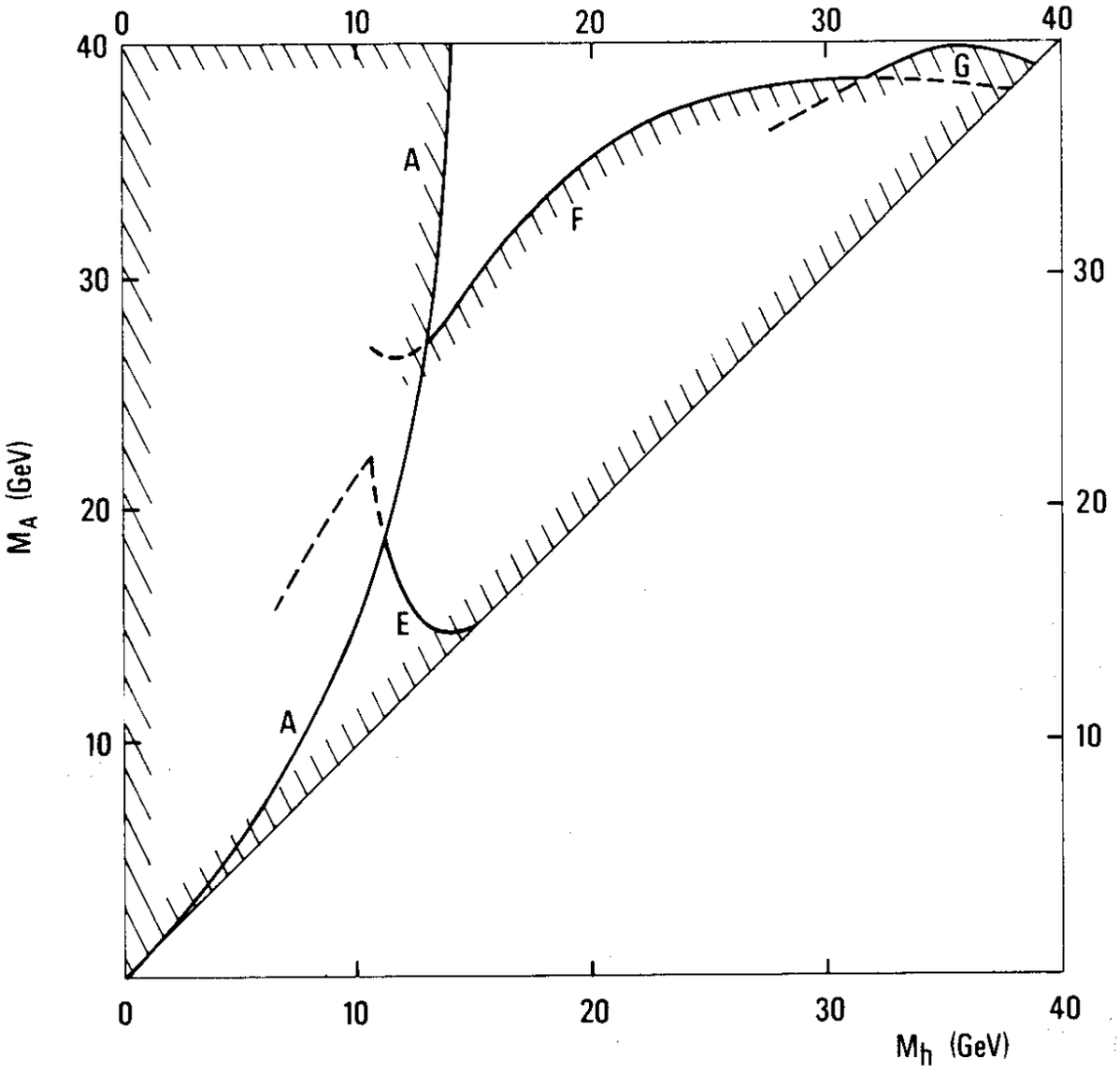

Figure 4.

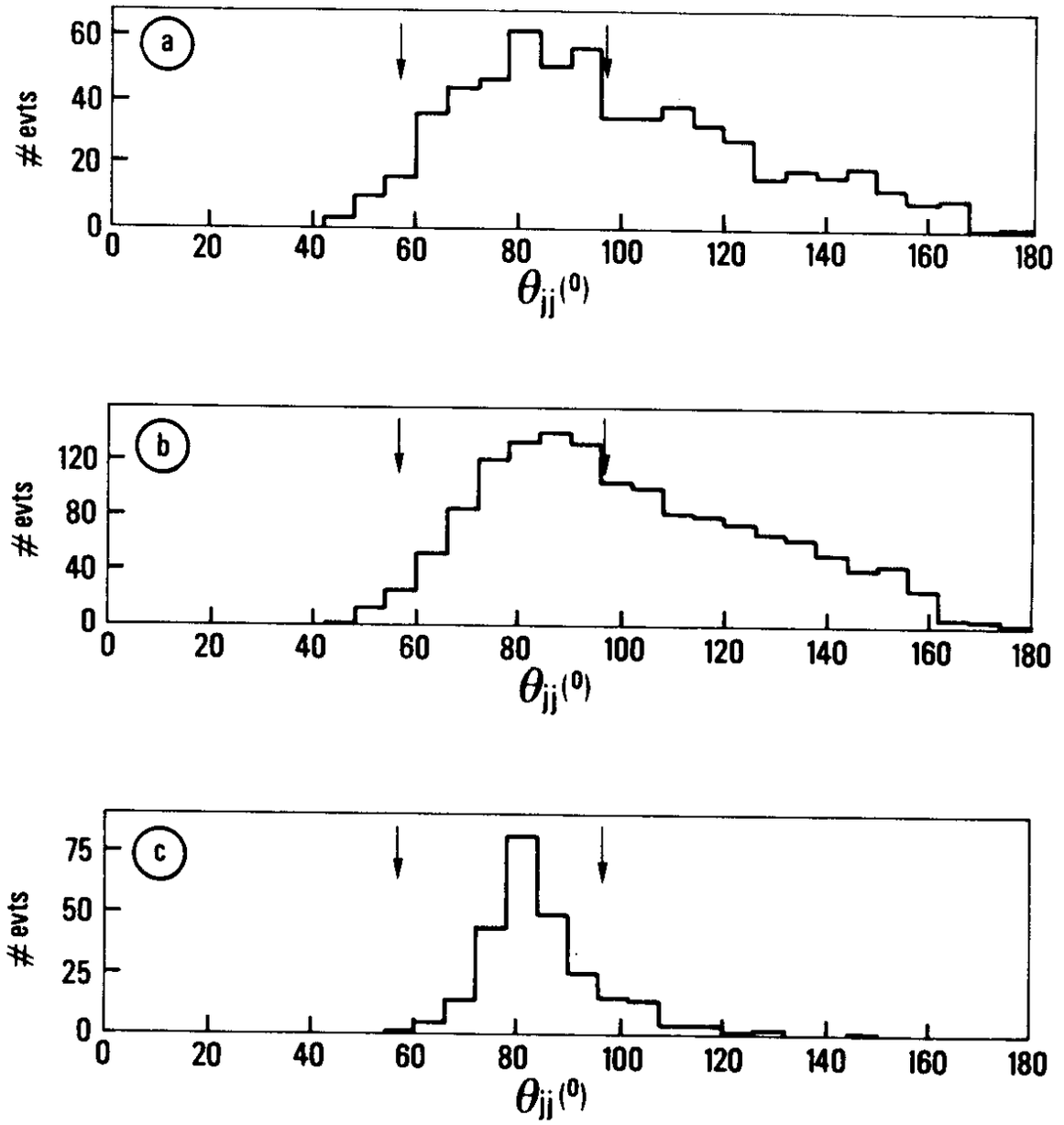

Figure 5.